



# Ecological risk assessment of heavy metals in riverine sediments of rural area driven by urbanization

Yi Zhou<sup>1</sup> · Shushu Guo<sup>1</sup> · Wanping Zhang<sup>1</sup> · Yuankun Yang<sup>1</sup> · Bin Wang<sup>1</sup> · Jingping Zhu<sup>1</sup> · Shu Chen<sup>1,2</sup> 

Received: 20 August 2022 / Accepted: 9 July 2023 / Published online: 24 July 2023  
© The Author(s), under exclusive licence to Springer-Verlag GmbH Germany, part of Springer Nature 2023

## Abstract

Rural revitalization denotes the gathering of large populations in rural areas and the subsequent gradual urbanization. Rural environments have been deteriorated by heavy metals (HMs) over the last few years. Without the existence of large-scale industries, the accumulation of HMs in sediments due to population aggregation in rural environments needs to be scientifically confirmed. Therefore, in this study we first understand the sediment pollution in rural environments in China and across the globe, and subsequently investigate HMs in sediments in rural micro water. The study area, Sichuan Province, China, was divided into two areas, namely, sparsely populated areas (SPA) and densely populated areas (DPA). Eight typical HMs (As, Zn, Ni, Hg, Cd, Cr, Cu, and Pb) were selected to target in riverine sediments, and the content and spatial distribution characteristics were analyzed. The results indicate that As, Hg, Cd, and Pb concentrations in sediments were higher than background values (BVs), with high concentration sample sites located in the DPA. In addition, the geo-accumulation index ( $I_{geo}$ ), pollution load index (PLI) and potential ecological risk index (RI) were used to quantitatively evaluate the pollution characteristics of HMs in sediments, revealing that the sediments exhibited high As and Hg pollution in the DPA (PLI=1.09). In general, mild (RI=48.76) and moderate (RI=154.92) HM pollution was observed in the sediments of the SPA and DPA, respectively, based on the high PLI (>1.0) and RI (>150) values. Correlation analysis and principal component analysis (PCA) indicate that the Cd in the sediment generally originated from geogenic sources, while the other elements (Zn, As, Cu, Cr, Hg, Ni and Pb) were primarily linked to anthropogenic sources. Finally, the results demonstrate that population aggregation will lead to the enrichment of HMs.

**Keywords** Rural environment · Heavy metals · Population aggregation · Ecological risk assessment · Sediment · Sichuan province

## Introduction

Heavy metals (HMs) are refractive, accumulate easily, and have strong stability in water and sedimentary environments, with heavy biological activity and toxic effects (Mirzaei et al. 2020). In addition, HMs can endanger the health of organisms through biological enrichment and food chain

amplification, and have consequently become a key pollutant affecting the environments of rivers and lakes (Zhang and Karimi-Maleh 2023b). Some studies have mentioned that metal ions such as  $Pb^{2+}$  and Cr(VI) in the water environment are the main pollutants, which are highly toxic to animals, plants and humans, have potential carcinogenicity, and pose a serious threat to the ecological environment (Karimi-Maleh et al. 2021; Zhang and Karimi-Maleh 2023a). As an important carrier of pollutants, sediments can indicate the pollution characteristics of the basin, and reflect the long-term impact of natural factors and human production activities on the environment. (Hong et al. 2020). (Tian et al. 2020) assessed the pollution of HMs in sediments and waters from 119 rivers, estuaries and marine sites in the Bohai Sea and the Yellow Sea in 2020, and conducted a comparative assessment between China and South Korea. Although scholars have evaluated large lakes and rivers in China,

Responsible Editor: Christian Gagnon

✉ Shu Chen  
crick\_chen@hotmail.com

<sup>1</sup> The Key Laboratory of Solid Waste Treatment and Resource Recycle, Ministry of Education, Southwest University of Science and Technology, Mianyang 621010, PR China

<sup>2</sup> School of Environment and Resource, Southwest University of Science and Technology, Mianyang 621010, China

under the current urbanization background, the impact of HMs in the surface sediments of rural micro-waters on rural ecological environments and human health remains unclear.

Following decades of reform, the opening-up of the economy, and a rise in population, China's urban structure has undergone tremendous changes. In particular, rural areas have gradually entered the stage of urbanization. (Xiao et al. 2013) analyzed and compared the spatial distribution, pollution level, toxicity and ecological risk level of Cd, Cr, Cu, Ni, Pb and Zn in sediment samples of two typical urban and rural rivers in the Pearl River Delta. The results revealed that the potential ecological risk index of rural river sediments was equal to that of urban river sediments, indicating the urgency to solve the ecological health problems of rural rivers in underdeveloped areas. (Jiang et al. 2017) collected 105 soil samples from a town in southern Jiangsu and detected the concentrations of 15 metal elements. The authors determined the accumulation of Cr, Cu, Cd, Pb, Ni and Co in the soil, with total risk indexes of 3.62 and 6.11, respectively, indicating mild pollution. The total risk of adults was  $9.78 \times 10^{-4}$  and that of children was  $4.03 \times 10^{-4}$ , while the non-carcinogenic and carcinogenic risks of soil metals were higher than the acceptable levels. More attention must be focused on chromium and arsenic, since their respective health risks exceed acceptable levels. The afore mentioned studies clearly demonstrate the gradual deterioration of the rural water environment, with data on water environment related indicators presenting greater pollution levels. Therefore, there is an urgent need to investigate the status of HM pollution in sediments and water, and assess the corresponding ecological risks.

As well as evaluating the HMs in the study area, numerous studies have also investigated the relationship between HMs and other factors. For example, based on surface soil samples (0–10 cm) from 238 sampling sites, (Argyrazi and Kelepertzis 2014) determined significant correlations between HM concentrations and urbanization indicators (e.g., traffic, urban land use, population density and urbanization time). Bo et al. (2015) divided the Taihu Lake region into three components: mixed areas (industrial and commercial), residential areas and agricultural areas and compared the respective HM content in sediments to reveal the following trend: mixed area > residential area > agricultural area. (Bo et al. 2015). (Zhang et al. 2017) assessed HM (Cr, Cu, Ni, Pb, and Zn) pollution and risks in the mountainous urban-belt (MB), mountain–plain urban-belt (MPB), and plain urban-belt (PB) areas of Haihe Basin. The authors concluded that the potential risks posed by the HMs (based on HM chemical fractions) generally decreased in the order MPB > MB > PB. Most scholars have evaluated the risk of heavy metal pollution in different functional areas of soil and sediments, or compared their enrichment degrees. However, in surface sediments of water bodies, what is the relationship between population density and heavy metals in surface sediments remains to be confirmed.

In the current study, we aim to: (1) investigate the distribution of HMs in the surface sediment of a rural environment without point source pollution containing HMs (e.g., the chemical industry); (2) predict the distribution of HMs in rural surface sediments in Sichuan under the same conditions; (3) assess the ecological risk of HMs; and (4) explore the relationship between population aggregation and HM deposition. The results provide a scientific basis for rural environments to control the risk of HMs. They also act as a reference for rural environmental protection and environmental planning and management, in response to the “rural revitalization” slogan.

## Materials and methods

### Description of the study area

Anyue County (104°56'51"—105°45'14" east longitude and 29°40'32"—30°18'53" north latitude), belonging to Ziyang City of Sichuan Province, is located in the central region of Sichuan Basin. It is a hilly agricultural county with a high population in the middle of Sichuan Basin, known as "the hometown of lemon in China" as it is the main production base of lemon products in China. Yueyang River is the main river in the territory. The entire basin of the Yueyang River covers 694.63 km<sup>2</sup>, including 635.16 km<sup>2</sup> in Anyue County, with a total length of 108.3 km and 59.56 km, respectively. As a tributary of the right bank of the Fujiang River system in Sichuan Province, the basin runs through Lezhi County, Anyue County of Ziyang City, Tongnan District of Chongqing, and finally flows into Fujiang. The basin runs through towns and urban areas, and land uses of surrounding land are mainly forestry, agriculture and breeding industries, which is a typical small-town watershed in Sichuan Province.

### Sampling and chemical analysis

A total of 17 surface sediments were collected from 17 uniformly distributed sampling sites in 2021 (Fig. 1). Based on the degree of population aggregation and geographical characteristics, the study area was divided into two regions. The first region is the densely populated area (DPA), which includes seven sampling points (S5, 6, 7, 8, 9, 10, and 15). The DPA belongs to the urban center with a large population, small-scale repair industries, restaurants, etc. The residents typically use coal heating in winter. The second region is the sparsely populated area (SPA), which includes seven sampling points (S1, 2, 3, 4, 15, 16, and 17). The region is characterized by a small population, numerous fisheries, animal husbandry, and lemon bases. All sampling sites collected from key pollution sources and river confluences were geographically located by global positioning system receivers. A grab type mud picker was employed to remove as much water as possible, and the mud samples in contact

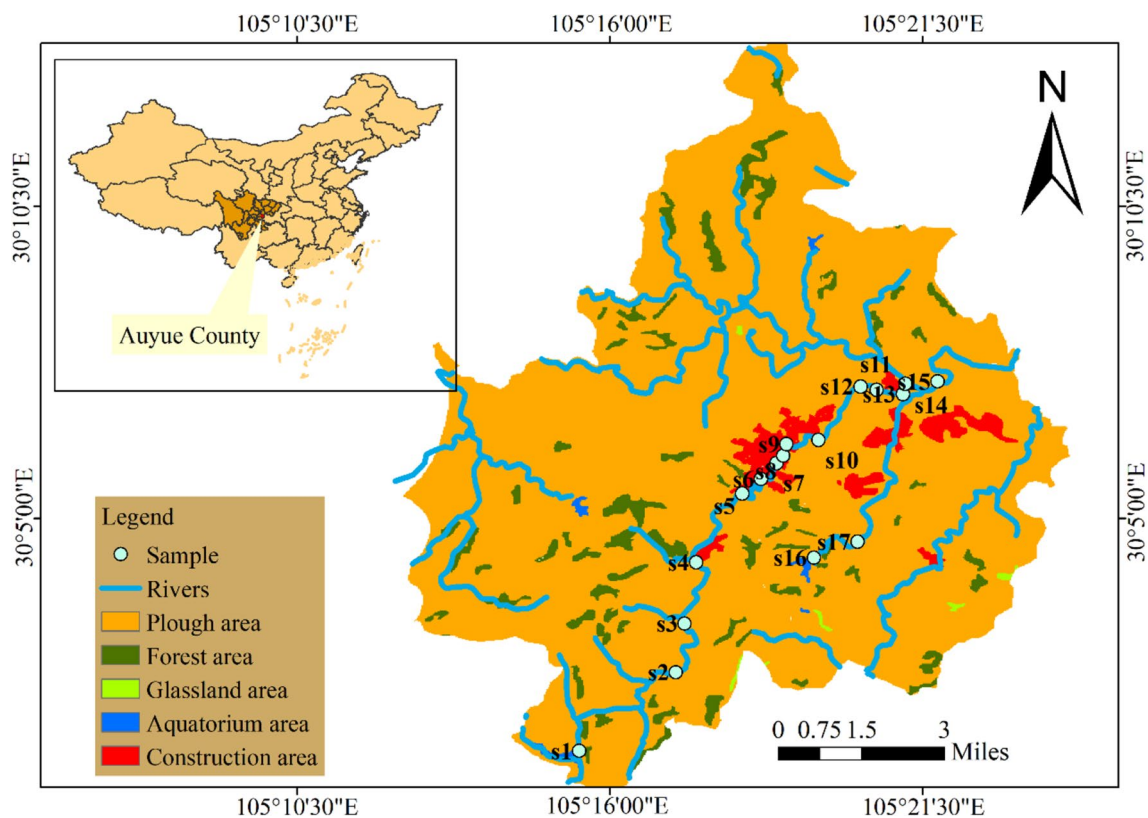


**Fig. 1** Location and sampling point of the study area (SPA: the sparely populated area; DPA: the densely area; s11, s12, s13: upstream, outlet and downstream of the sewage treatment plant)

with the sampler were removed, as was debris, vegetation etc. The mud samples were placed into thoroughly cleaned plastic bags, transported to the laboratory, and stored with dry ice during the experiment. (Dash et al. 2020; Sundaray et al. 2011). The collected sediment samples were dried with a freeze dryer (Free Zone 6 Liter, USB, Labconco) and grinded through a fine 75  $\mu\text{m}$  sieve to obtain the pre-treated samples. The samples were then packed in sealing bags for the subsequent analysis.

All sediments were digested with a concentrated acid mixture [HCl (6 mL)-HNO<sub>3</sub> (2 mL)-HF (4 mL)] in a polytetra-fluoroethylene container. The concentrations of Cd, Cr, Cu, Pb, Zn and Ni in the digestion solution were determined by inductively coupled plasma-mass spectrometry (X7 Quadrupole ICP-MS, American Thermo Scientific), and the contents of As and Hg were determined by atomic fluorescence spectrometry (AFS, Beijing Jitian Instruments Co., Ltd. production, AFS-8X). (Tian et al. 2020).

### Quality assurance and quality control

A strict QA/QC program was adopted for the experiments. The standard materials for the composition analysis of the stream sediments (GBW07309) by the Institute of Geophysical and

Geochemical Investigation were used to improve the accuracy of the experiment, which were approved by the General Administration of Quality Supervision, Inspection and Quarantine of the People's Government of China. The recovery rates of Cr, Ni, Cu, As, Cd, Pb, Hg and Zn remained between 80.17% and 105.25%. Furthermore, a blank test was performed for each batch of experiments with three parallel samples. More specifically, experimental glassware was soaked in 15% HNO<sub>3</sub> (w/w) for at least 24 h prior to being used and subsequently soaked and rinsed with deionized water. All experimental reagents were of analytical grade or higher.

### Sediment's contamination and risk assessment indices

#### Geo-accumulation index

The geo-accumulation index (Tunca et al. 2018) not only reflects the natural variation characteristics of HM distribution, but can also distinguish the impact of human activities on the environment. (Guo et al. 2018). In addition, the influence of background values (BVs) caused by natural geological processes is considered in order to fully consider the influence of human activities on HM pollution as follows:

$$I_{geo} = \log_2 \left[ \frac{C_n}{kC_{Bn}} \right] \tag{1}$$

Where  $C_n$  is the measured concentration of the metal in sediment  $n$ ;  $C_{Bn}$  is the geochemical background value of element  $n$  and factor; and  $k$  is the coefficient variation of the background data due to lithogenic impacts ( $k = 1.5$ ). Table 1 reports the classification of the HM pollution degree in the sediments into seven grades by the geo accumulation index.

**Pollution load index (PLI)**

$I_{geo}$  and pollution index (PI) are used to evaluate and analyze pollution levels based on a single HM, while the PLI provides comprehensive information about the risks caused by the existence of multiple metals (Ali et al. 2018), and can thus make a more comprehensive evaluation of HM pollution (Celis-Hernandez et al. 2020). PLI is determined as the  $n$ th root of the product of  $n$  PI Potential ecological risk index method:

$$PI = \frac{Cn}{CB} \tag{2}$$

$$PLI = \sqrt[n]{PI_1 \times PI_2 \times \dots \times PI_n} \tag{3}$$

Where  $Cn$  is the concentration of the tested HM;  $CB$  is the background concentration of the HM;  $Cf$  is the contamination factor; and  $n$  is the number of metals. If  $PLI > 1$ , then pollution is present; otherwise, no metal pollution is detected.

**Assessment of potential ecological risk**

The potential ecological RI, proposed by (Hakanson 1980), is used to assess the comprehensive pollution status in the sediments and environmental effects based on toxicology (Huang et al. 2020). The relevant equations are described as follows:

$$EI = T_i \times PI_i \tag{4}$$

$$RI = \sum_{i=1}^n EI \tag{5}$$

Where  $T_i$  denotes the toxicity effect coefficient, with values of  $Cd = 30$ ,  $As = 10$ ,  $Pb = Cu = Ni = 5$ ;  $Cr = 2$ ; and  $Zn = 1$ ;  $PI_i$  is the single pollution index of a given metal; and  $RI$  is the ecological hazard risk. Table 1 reports the five EI and RI grades of the HMs.

**Data analyses**

The HM concentrations in the sediments were evaluated using descriptive statistics (e.g., including mean, median, standard deviation and coefficient of variation). Spatial analysis and concentration comparisons were carried out to understand the spatial distribution characteristics of the HMs, and to determine the significant difference of HM concentrations between different regions and land use types. Multivariate analysis techniques, such as Pearson correlation analysis and principal component analysis (PCA), were employed to analyze the relationship among HMs in sediments and to interpret the possible sources of the HMs. The relationship between HM concentration and population was described by a waterfall diagram. SPSS Statistics 25 (IBM) was used to perform the statistical analyses. The spatial distributions of the HM concentrations and the  $I_{geo}$ , PLI and RI indexes were visualized with ArcGIS 10.8 (Esri).

**Results and discussions**

The results are divided into the following four sections: (1) understanding the distribution characteristics of the total amount of HMs in the surface sediments of the study area; (2) evaluating of the ecological risks in the study area; (3) determining the possible origins of the HMs; and (4) exploring the relationship between HM concentration and population concentration.

**HM concentrations in sediments**

Table 2 reports the HM contents in the surface sediments of Yueyang River and the corresponding reference standard for

**Table 1** Different pollution risk indexes and their grades

Class	Geo-accumulation index ( $I_{geo}$ )	Pollution status	EI	Risk level	RI	Potential ecological hazard
0	$I_{geo} < 0$	Unpolluted	$EI < 40$	Weak	$RI < 150$	Low
1	$0 < I_{geo} < 1$	Mildly	$40 \leq EI < 80$	Medium	$150 \leq RI < 300$	Modetate
2	$1 < I_{geo} < 2$	Uppolluted to moderately	$80 \leq EI < 160$	Considerable	$300 \leq RI < 600$	Considerable
3	$2 < I_{geo} < 3$	Moderately polluted	$160 \leq EI < 320$	Strong	$RI \geq 600$	very high
4	$3 < I_{geo} < 4$	Moderately to strongly polluted	$EI \geq 320$	Extremely strong	/	/
5	$4 < I_{geo} < 5$	Strongly polluted	/	/	/	/
6	$I_{geo} > 5$	Strongly to extremely polluted	/	/	/	/

the whole study area. Sampling point concentrations below the detection limit were recorded as 0. Due to the lack of relevant standards for HMs in river sediments in China, the soil background value of Sichuan was chosen as a reference. Despite the lack of large-scale industrial pollution sources close to the study area, compared with the soil background value in Sichuan, the HMs in the surface sediments of Yueyang River were elevated, with the exception of Cr. As, Cd, Pb and Hg were elevated by more than 35% of the sampling points, while this value was less for Ni, Cu and Zn. The mean concentrations of As and Hg were approximately 36.31% and 5.24% higher than their BVs, respectively. The maximum accumulation of As, Cd and Hg in the sediments were observed as 72.3071, 0.1511 and 0.3882 µg/g, exceeding the BVs by 595.26%, 385.26, and 151.82%, respectively. The concentrations of the other elements (Cd, Pb) did not exceed, or were close to, their BVs. As and Cd exhibited the highest coefficient of variation (> 140.0%), followed by Zn (> 70.0%).

Compared with previous studies, the heavy metal content of surface sediments in relevant rural waters was compared (Liu et al. 2009; Xia et al. 2020; Yan et al. 2020). It can be seen from Table 3 that the concentration of HMs in C was lower than that in other places except Cu. Since the sampling time in C was in 2009, it can be further explained that the enrichment of heavy metals in

surface sediments in rural waters is becoming more and more serious, which may be the result of urbanization. At the same time, we also found that the enrichment degree of heavy metals in this study area was almost the same as that of D and E, because the surrounding environment of the study area was similar and there was no large industrial industry. However, the concentrations of all heavy metals except Cu in site B were higher than those in other places, which may be due to the greater urbanization in Guangdong.

In order to better understand the distribution of HM concentrations in the study area, the results were grouped and compared according to our field records, sampling locations and spatial distribution of HMs in sediments and subsequently (Fig. 2). As, Cd, Hg, Ni and Pb were mainly distributed in the central part of the river. The sampling points in this section were mainly in the densely populated areas, and the HMs were generally from anthropogenic emissions. Among them, As, Cd and Hg exhibited the most elevated values, and there were significant differences in upstream and downstream concentrations. This may be attributed to population aggregation. The enrichment of other elements (Cr, Cu and Zn) was moderate, with the corresponding concentrations evenly distributed across the river and no large differences. Note that in

**Table 2** Heavy metal contents in sediments of Yueyang River

Sampling site	AS (µg/g)	Cd	Pb	Cr	Ni	Cu	Zn	Hg
s1	N/A	0.0584	25.2976	55.4203	24.0161	23.5603	70.8667	0.0018
s2	N/A	0.0051	25.7381	55.8724	24.4212	28.6722	82.2333	0.0391
s3	N/A	0.0261	20.7454	48.6768	20.6074	18.9534	28.7333	0.0322
s4	N/A	0.0318	29.7146	59.4905	23.6426	27.2548	102.9667	0.0376
s5	72.3071	0.1051	32.3784	78.0401	35.0967	26.0274	70.6333	0.0454
s6	47.6367	0.2252	36.4722	69.3063	31.0211	28.7194	126.3000	0.0391
s7	23.3452	0.0051	34.6264	47.7370	17.8036	30.7339	85.7333	0.0882
s8	35.0204	0.1730	48.8228	55.9815	24.8636	24.9184	69.4500	0.0863
s9	11.4566	0.1176	36.6921	54.0234	20.3136	34.7353	139.5667	0.0942
s10	8.9861	0.0807	37.5890	61.8523	24.0482	29.8081	69.0000	0.0581
s11	0.5687	0.0130	20.7550	58.2722	18.7155	18.1390	18.3000	0.0640
s12	N/A	N/A	22.2333	53.5015	24.8616	24.4860	4.7000	0.1511
s13	3.2630	N/A	21.7055	49.7074	20.5887	19.4835	9.2667	0.0438
s14	38.4111	0.3882	27.3263	66.7054	29.6801	21.4566	4.2000	0.0804
s15	N/A	N/A	20.6610	42.5635	24.9820	14.6184	56.5667	0.1155
s16	N/A	N/A	11.0778	19.5316	8.2686	6.4609	N/A	0.0373
s17	N/A	N/A	24.1677	61.5507	26.7439	16.9863	N/A	0.0595
BV	10.4	0.08	30.9	79.0	32.6	31.1	86.5	0.06
Mean	14.1761	0.0723	28.0001	55.1901	23.5102	23.2361	55.2068	0.0631
SD	21.0755	0.1026	8.6930	12.2021	5.7468	6.7562	43.6658	0.0350
CV	148.67%	141.98%	31.05%	22.11%	24.44%	29.08%	79.09%	55.43%
Min	0.5687	0.0051	11.0778	19.5316	8.2686	6.4609	4.2000	0.0018
Max	72.3071	0.3882	48.8228	78.0401	35.0967	34.7353	139.5667	0.1511

\*N/A, not detected



**Table 3** Comparison of heavy metal content in surface sediments in different rural rivers

Locations	Metal concentrations (mg/kg)					References
	As	Cd	Zn	Cu	Pb	
Yueyang river, Sichuan(A)	14.17	0.07	55.20	23.24	28.00	This study
Rural river Guangdong(B)	28.27	1.95	212.28	68.20	86.90	(Yan et al. 2020)
Luan River, China(C)	7.49	0.03	23.38	92.54	23.47	(Liu et al. 2009)
Rural reservoir river, Wuhan(D)	6.53	0.50	105.75	105.45	32.59	(Xia et al. 2020)
Rural commercial fishing river, Wuhan(E)	10.04	0.32	95.97	37.37	29.51	

the absence of the fishery industry in the upstream (the source of a large amounts of Cu), the Cu concentration in the middle reaches of the river may have been quite different to that in the upstream. (Li et al. 2017; Rodriguez Martin et al. 2006) Sampling point 14 exhibited relatively high and irregular HM concentrations compared to the other sampling points. This is due to its location in another intersection river that was seriously polluted by point sources, and it also belongs to the population aggregation area. Downstream of the river, all elements except Hg were less enriched. This is attributed to a sewage treatment plant at the sampling points (S11–S13) in this section, where artificial floating islands and other water purification equipment were set to reduce the concentrations of pollutants.

In general, HM concentrations were higher in the populated areas. Moreover, the HMs concentrations varied greatly, and these differences may not reflect the actual pollution levels due to the existing spatial heterogeneity in sediments. Therefore, the HM assessment in the sediments cannot only be assessed simply with the HM concentrations. Other ecological indicators ( $I_{geo}$ , PI, PLI, RI, etc.) should be required to account for the BVs in the corresponding riverine sediments.

### Assessment of pollution levels and potential ecological risk in sediments

The average  $I_{geo}$  values of all HMs were less than zero, indicating that the accumulation of HMs throughout the basin was mild. The average  $I_{geo}$  values of the SPA area was less than 0, denoting an “unpolluted” contamination level. In contrast, the average  $I_{geo}$  value of As in the DPA area was 0.62, indicating “high As contamination”. Figure 3 depicts the spatial distribution of the  $I_{geo}$  values for the HMs in surface sediments. The peak  $I_{geo}$  values of As, Cd, Pb, Cr, Ni, Cu, Zn and Hg were determined as 2.21, 1.71, 0.07, -0.60, -0.48, -0.43, 0.11 and 0.72, respectively, and were located in DPA. This suggests the high HM pollution levels in the DPA. However, the  $I_{geo}$  values of all HMs were less than 0 in the SPA, indicating the relatively low HM risks in the sediments of this area. Compared with the  $I_{geo}$  values of rural rivers in Guangdong Province, the

$I_{geo}$  values of heavy metals in rural rivers in Guangdong Province were greater than those in the study area. More importantly, the  $I_{geo}$  value of Cd showed “strongly polluted” ( $4 < I_{geo} < 5$ ) (Yan et al. 2020). This may be related to industrialization and rapid urbanization, because the main source of Cd is industry (Yi et al. 2016).

The PI values ranged from 0 to 6.95, 0–4.91, 0.36–1.58, 0.25–0.99, 0.25–1.07, 0.21–1.12, 0–1.61 and 0.03–2.47 for As, Cd, Pb, Cr, Ni, Cu, Zn and Hg, respectively (Fig. 4). Hg, Cd and As exhibited the largest variation in the PI among the sediments, with values exceeding 1.0 in some sediments. The results suggest that sediments in the basin were polluted by these HMs. The PLI values of most sediments were greater than 1 in the whole study area, with the SPA and DPA values of surface sediments ranging between 0.31–1.11 and 0.72–1.35, respectively. Average PLI values in SPA and DPA were greater than 1, revealing the presence of HM pollution. In particular, the mean PLI values were 0.64 and 1.09, respectively, indicating that HM contamination existed in the DPA. The highest PLI value (1.3) was observed in sampling site S6 in DPA (Fig. 6). PLI values of other sampling sites in the DPA were all greater than or close to 1, indicating that the sediments were mildly polluted with the measured HMs.

Figures 5 and 6 reveal the EI values of all measured HMs in the sediments to exhibit the following trend in concentration: Hg > Cd > As > Pb > Cu > Ni > Cr > Zn in the whole study area, Hg > Cd > Pb > Ni > Cu > Cr > Zn > As in the SPA and Cd > Hg > As > Pb > Cu > Ni > Cr > Zn in the DPA. Furthermore, Hg and Cd posed the highest risks in the DPA, with average EI values > 40, suggesting “medium risk”. EI values of Cd in DPA were close to 901% of those in depopulated areas. RI values ranged from 29.05 to 175.46 (mean: 96.41) in the whole study area, 29.05 to 96.97 (mean: 48.76) in the SPA and 97.68 to 175.46 (mean: 154.92) in the DPA. the average RI value of the latter exceeded 150, indicating that all measured metals posed medium ecological risks. The maximum RI value (251.26) was observed at sampling site S14, denoting medium ecological risks (Fig. 6). Moreover, S5, S6 and S8 in the DPA exhibited high RI values (175.46, 173.87 and 156.79), corresponding to relatively high levels of human activities compared to S1, S2 etc. in the SPA with low RI values. At each sample point, the dominant

**Fig. 2** Spatial distribution of heavy metals in sediments in the study areas

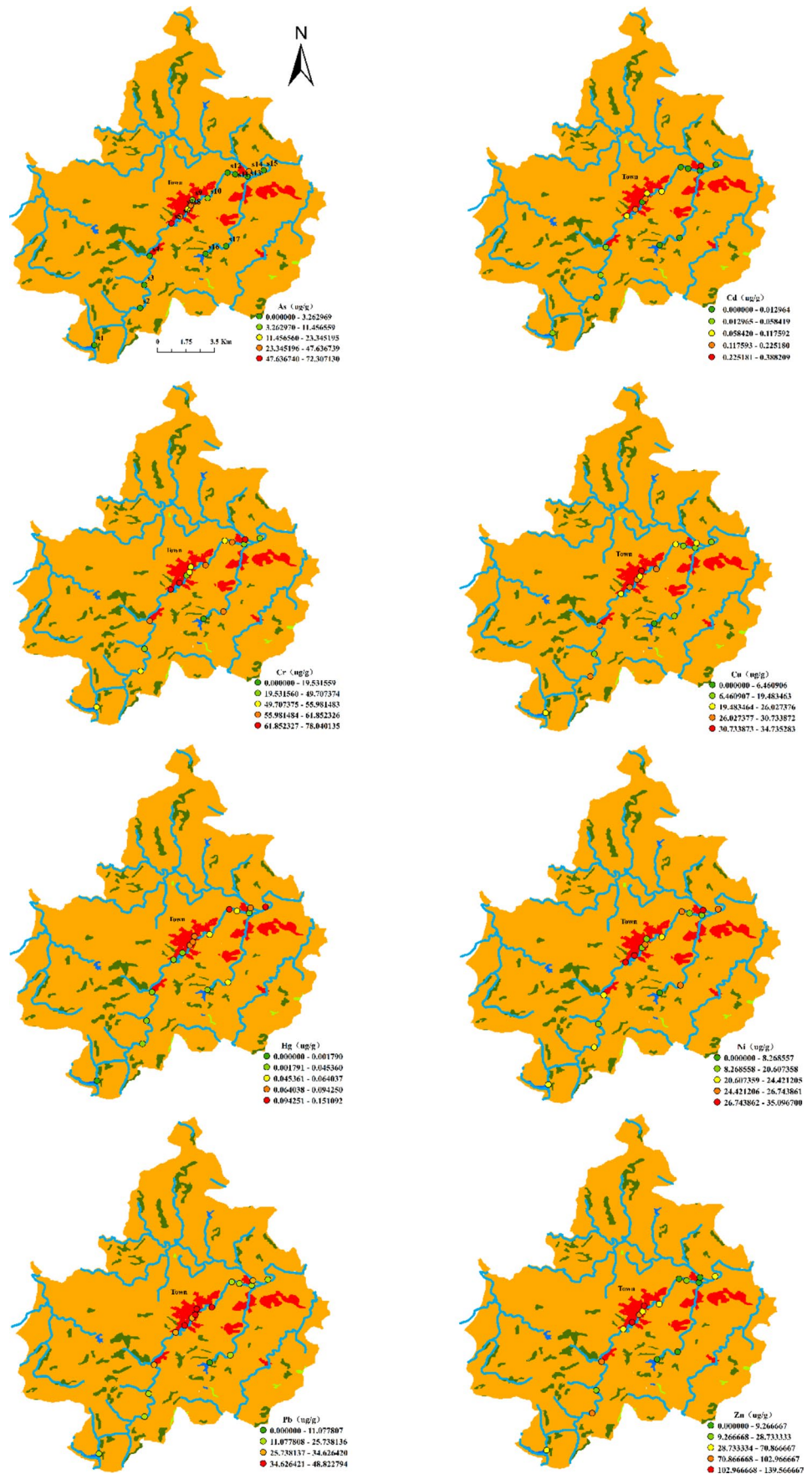


**Fig. 3** Spatial distributions of Igeo of heavy metals in sediments in the study areas

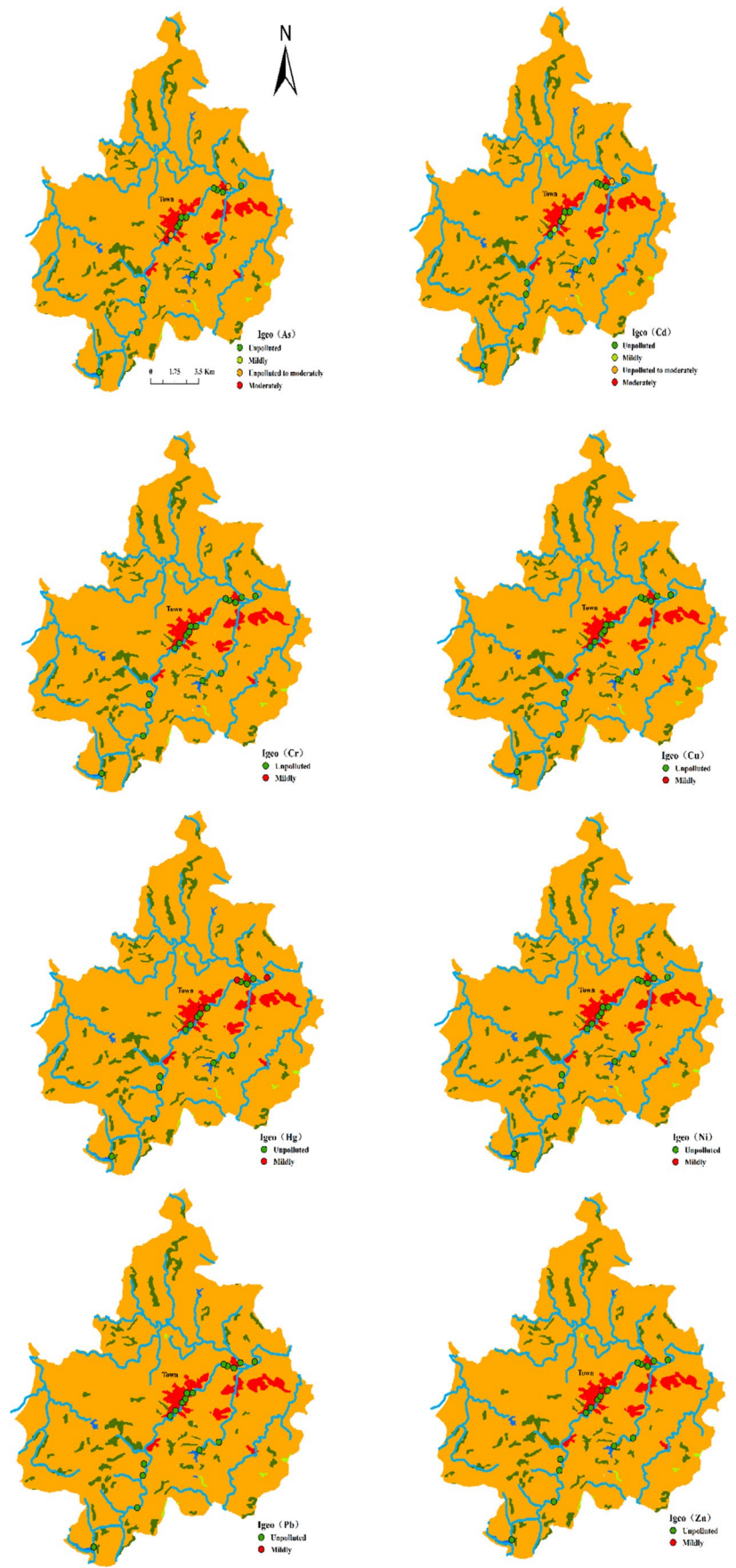
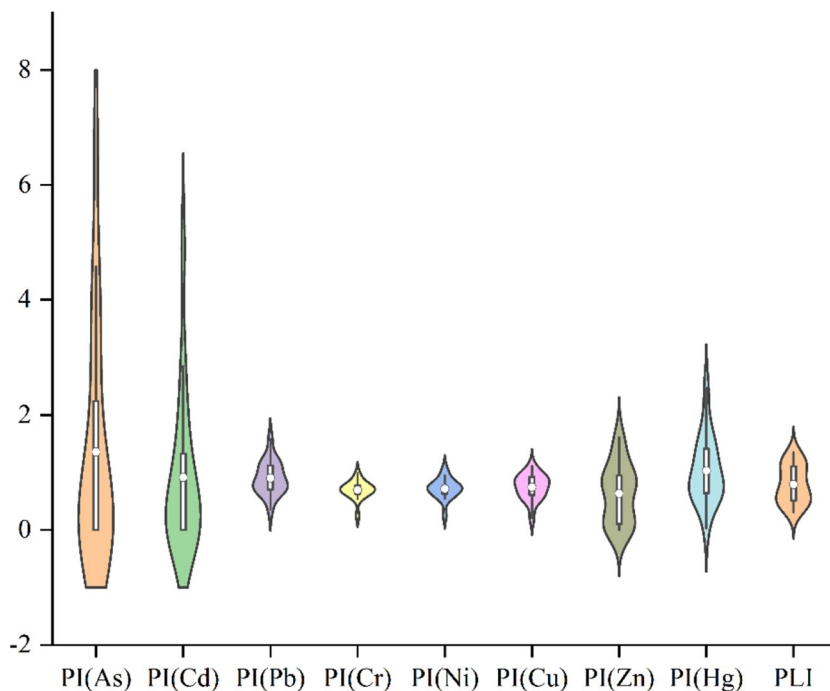




**Fig. 4** Violin plot and boxplot of heavy metal pollution index (PI) and PLI in sediments. Whiskers extend to the most extreme data point, which is no more than 1.5 times the interquartile range from the box. The white point represents the mean concentration of heavy metals



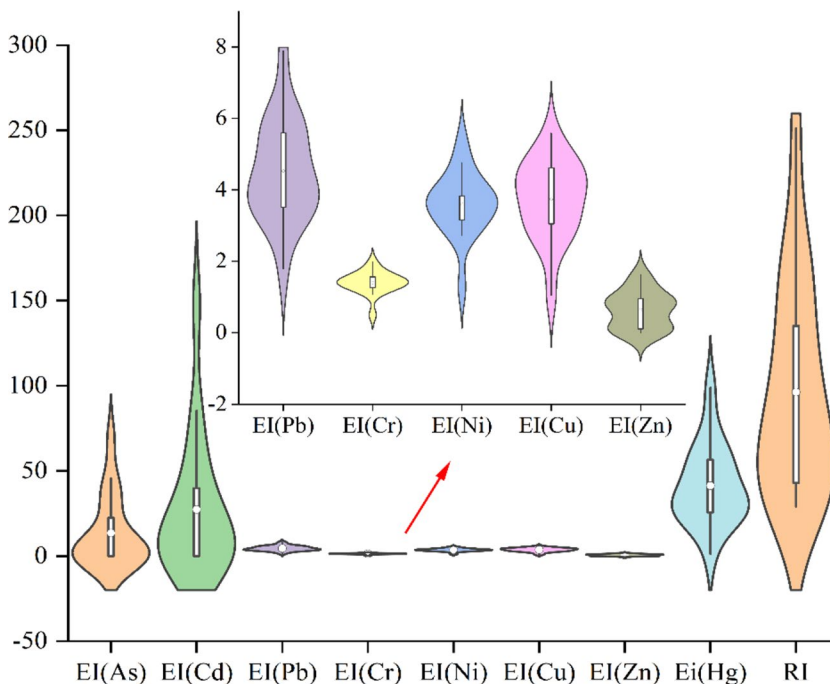
contributing factor of the potential ecological risk index was Cd. However, in the SPA, Hg was the main contributing factor. As also had a high contribution rate in the DPA.

**Source identification of the HMs in sediments**

Similar HM sources leads to a certain correlation between HMs. Therefore, correlation analysis is an important basis

in predicting the sources of HMs, and HMs with significant correlations may have the same sources. (Barkett and Akun 2018, Jiang and Guo 2019). Pearson correlation analysis of the HMs in the surface sediments of Yueyang River (Table 4) revealed a significant positive correlation among Ni, Cr and As ( $p < 0.01$ ). This implies that these three HMs may have the same source and similar migration and transportation paths. (Jin et al. 2019). Pb was positively

**Fig. 5** Violin plot and boxplot of heavy metal ecological index (EI) and RI in sediments. Whiskers extend to the most extreme data point, which is no more than 1.5 times the interquartile range from the box. The white point represents the mean concentration of heavy metals



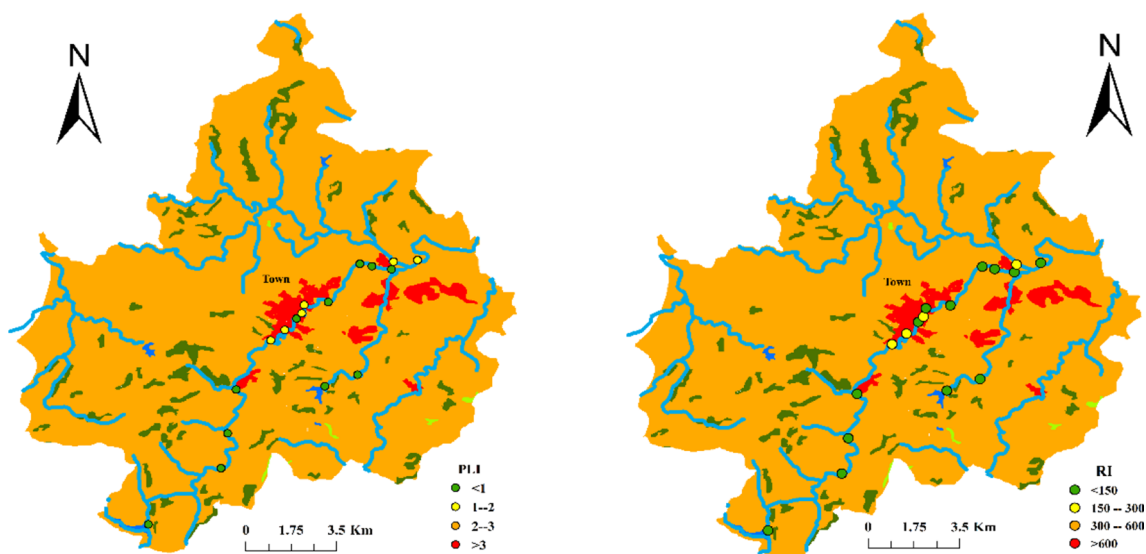


**Fig. 6** Spatial distribution of the pollution load index (PLI) and ecological risk index (RI) of heavy metals in sediments in the study areas

correlated with Cr ( $p < 0.05$ ) and As ( $p < 0.05$ ). Due to their similarity, it was speculated that Pb may have similar sources to Ni, Cr and As, yet Pb was not significantly correlated with Ni, indicating that Pb may have other sources. Significant positive correlations were observed between Pb, Zn and Cu ( $p < 0.01$ ), indicating that they may have the same source and similar migration and transport routes. Cr was positively correlated with Pb ( $p < 0.05$ ) and Cu ( $p < 0.05$ ). Again, the similarity between Pb, Zn and Cu suggests that Cr may have similar sources to these HMs. However, Cr was not significantly correlated with Zn, indicating distinct sources for Cr. There was no significant correlation between Cd and Hg and other HMs, indicating that Pb and Cr had their own unique sources.

Principal component analysis (PCA) reduces the dimension based on orthogonal transformation. It combines a set of possibly correlated variables into a set of linear unrelated variables and can be used to analyze whether HMs come from the same pollution source (Franco-Uria et al.

2009; Islam et al. 2018). The PCA of eight HMs in surface sediments of Yueyang River (Tables 4 and 5) determines variance contribution rates of PC1, PC2, PC3 and PC4 as 49.285%, 16.31%, 14.300% and 8.408%, respectively, with the cumulative variance contribution rates of the four principal components reaching 85.99% ( $> 85\%$ ). This indicates that the four principal components could sufficiently reflect the vast majority of information provided by their environmental indicators (Lin et al. 2016). Pb and Cr of PC1 exhibited large positive loads, both exceeding 0.8, and As and Ni also had large loads ( $> 0.7$ ), revealing these four HMs to have the same sources. This was consistent with the correlation analysis. The main source of Pb was coal combustion, and key sources Cr include the electroplating, metal smelting, mechanical manufacturing and chemical industries (Wang et al. 2020). However, there was no large industrial source in this study area, and relatively high Pb and Cr contents were observed for DPA. This area has numerous small auto repair businesses and coal is used

**Table 4** The relationship among the contents of heavy metal elements

	As	Cd	Pb	Cr	Ni	Cu	Zn	Hg
As	1							
Cd	0.328	1						
Pb	0.558*	0.228	1					
Cr	0.606**	0.457	0.543*	1				
Ni	0.633**	0.438	0.443	0.887**	1			
Cu	0.332	0.362	0.758**	0.582*	0.404	1		
Zn	0.299	0.297	0.654**	0.306	0.235	0.768**	1	
Hg	-0.010	-0.200	0.126	-0.072	0.050	0.100	-0.120	1

\*Significant correlation at  $p < 0.05$

\*\*Significant correlation at  $p < 0.01$

**Table 5** Results of principal component analysis of heavy metals in sediments

	Initial eigenvalue				Load			
	Eigenvalue	Percentage of variance	accumulation		PC1	PC2	PC3	PC4
PC1	3.943	49.285%	49.285%	As	<b>0.720</b>	-0.280	0.198	-0.369
PC2	1.305	16.318%	65.603%	Cd	0.560	-0.342	-0.366	<b>0.589</b>
PC3	1.144	14.300%	79.903%	Pb	<b>0.813</b>	0.390	0.098	-0.192
PC4	0.673	8.408%	88.310%	Cr	<b>0.852</b>	-0.355	0.120	-0.018
PC5	0.485	6.061%	94.371%	Ni	<b>0.782</b>	-0.455	0.263	0.013
PC6	0.247	3.086%	97.457%	Cu	0.460	<b>0.811</b>	-0.083	0.153
PC7	0.157	1.962%	99.418%	Zn	0.545	<b>0.674</b>	-0.367	-0.034
PC8	0.047	0.582%	100.000%	Hg	-0.013	0.341	<b>0.858</b>	0.357

for heating, resulting in metal entering the water through domestic sewage. This suggests that the sources of Pb and Cr were domestic sewage.

Zn and Cu had large loads in PC2, (0.811 and 0.674, respectively), while the loads of other HMs were small. PC2 can be considered as an agricultural source due the high contribution of Cu and Zn, as the use of fertilizers is typically associated with the enrichment of Cu and Zn in the environment. (Li et al. 2020; Maanan et al. 2015). In summary, it was speculated that PC2 was an agricultural source.

Hg exhibited a large load in PC3 (0.858), while the remaining HM loads were small. This is consistent with the correlation analysis that implies unique Hg sources. The proportion of Hg concentrations greater than BV was low, while the Igeo suggested no pollution, indicating a low human influence, and thus a natural source is speculated for Hg (Chaturvedi et al. 2018; Chen et al. 2019).

In PC4, Although the variance contribution rate of PC4 was only 8.408%, Cd had a large positive load of 0.589, while other HM loads were small. This further verifies the unique sources of Cd suggested by the analysis results. The study region contains many lemon industrial bases. The HM detection data in the local soil reveals that just a small amount of Cd was enriched, and the concentration was lower than the BV. This implies that Cd only originated from HMs in the soil of lemon bases.

### Relationship of HMs and population aggregation

By combining the analysis of the HM concentrations, and the Igeo, PI, PLI, EI, and RI values, we can briefly conclude that: (1) the concentration of HMs in sediments in the DPA was markedly higher than that in the SPA; and (2) the average values of PLI, EI, and RI of HMs in DPA were higher than those in SPA, particularly for As, Pb, and Hg. Among them, the average EI value of As in DPA was 901.14% that of SPA. The results indicate the higher potential HM risks of DPA compared to SPA.

In recent years, with the development of urbanization has been followed by the expansion of heavy industries in cities. Previous studies have shown that the level of urbanization may lead to more serious Cr and Zn pollution in urban river sediments (Zhang et al. 2017). Ariadne Argyraki et al. found a significant indigenous correlation between concentrations of HMs in soil and urbanization indicators, including vehicle traffic, urban land use, population density and urbanization time (Argyraki and Kelepertzis 2014). In order to gain more insight into the influence of urbanization on HM pollution in soil, we divided the study area into two regions (SPA and DPA), both of which were not affected by heavy industry to discuss the relationship between population density and heavy metals in sediments. Figure 7 reveals the obvious enrichment of As, Cr, Zn, Pb, Cd and Hg in the DPA, with an inverted V-shaped shape indicating that

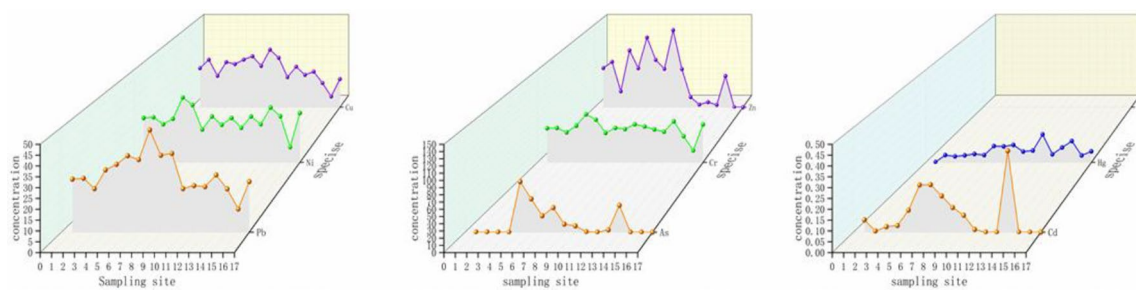


**Fig. 7** The waterfall figure (Represent the concentration trend of each heavy metal)

the concentration in DPA was higher than that in SPA. The variations in Ni and Cu concentrations were relatively moderate, with no large differences in concentration. The field sampling analysis and local land use types reveal the lack of heavy industry in the study area, while the fishing, animal husbandry and lemon industries dominate. The feed in the fishing and animal husbandry industries contain high Cu levels, which may explain the limited variation in the Cu concentration (Mendiguchía et al. 2006; Rodríguez Martín et al. 2006). The key difference between the SPA and DPA is the degree of population agglomeration. The results demonstrate the concentration of HMs (As, Cr, Zn, Pb, Cu, Cd and Hg) in rural water sediments to be significantly correlated with population agglomeration.

## Conclusions

The present study comprehensively investigated the spatial distributions and potential ecological risks of HMs in the rural water sediments of the SPA and DPA. The influence of population aggregation on HM pollution was then investigated. The conclusions we draw are as follows:

- (1) The spatial distribution of the HMs showed that the average concentrations of As and Hg exceeded the BVs. The mean concentrations of As and Hg were approximately 36.31% and 5.24% higher than their BVs, respectively. The spatial distribution was observed to vary across HMs, and with the exception of Cu and Ni, the HMs were concentrated in the DPA.
- (2) Average Igeo values of the HMs were less than zero, apart from As in the DPA, with a Igeo value of 0.618. As and Cd accumulation was detected in the DPA. Average PLI (> 1.0) and RI (> 150) values indicated the sediments in the study area to be mildly contaminated with the HMs.
- (3) Correlation and principal component analyses showed that without heavy industry, the following four sources can be identified for the pollution observed in the rural surface sediments under the background of urbanization: domestic sewage, agricultural source, natural source and crop farming.

This is confirmed by the positive relationship between population aggregation and HM concentration. The results of this study are a useful reference for environmental agencies or governments to monitor and manage HMs in the surface sediments of rural environments from a long-term perspective.

**Author contribution** Yi Zhou: Writing-original draft, Data curation. Shushu Guo, Wanping Zhang: Investigation, Data curation. Yuankun

Yang, Bin Wang, Jingping Zhu: Supervision, Methodology. Shu Chen: Methodology, Writing—review & editing. All the authors read and approved the final manuscript.

**Funding** This work was supported by the Youth Science Foundation of the National Natural Science Foundation of China (42107481), the Key Research and Development Project of Sichuan Science and Technology (2021YFS0289), and the Research Foundation of Southwest University of Science and Technology (20ZX7150).

**Data availability** Not applicable.

## Declarations

**Ethical approval** Not applicable.

**Consent to participate** Not applicable.

**Consent to publish** Not applicable.

**Competing interests** The authors declare no competing interests.

## References

- Ali AE, Strezov V, Davies PJ, Wright I (2018) River sediment quality assessment using sediment quality indices for the Sydney basin, Australia affected by coal and coal seam gas mining. *Sci Total Environ* 616:695–702
- Argyriaki A, Kelepertzis E (2014) Urban soil geochemistry in Athens, Greece: the importance of local geology in controlling the distribution of potentially harmful trace elements. *Sci Total Environ* 482:366–377
- Barkett MO, Akun E (2018) Heavy metal contents of contaminated soils and ecological risk assessment in abandoned copper mine harbor in Yedigöller, Northern Cyprus. *Environ Earth Sci* 77:378
- Bo LJ, Wang DJ, Li TL, Li Y, Zhang G, Wang C, Zhang SQ (2015) Accumulation and risk assessment of heavy metals in water, sediments, and aquatic organisms in rural rivers in the Taihu Lake region, China. *Environ Sci Pollut Res* 22:6721–6731
- Celis-Hernandez O, Giron-Garcia MP, Ontiveros-Cuadras JF, Canales-Delgado JC, Perez-Ceballos RY, Ward RD, Acevedo-Gonzales O, Armstrong-Altrin JS, Merino-Ibarra M (2020) Environmental risk of trace elements in mangrove ecosystems: an assessment of natural vs oil and urban inputs. *Sci Total Environ* 730:138643
- Chaturvedi A, Bhattacharjee S, Singh AK, Kumar V (2018) A new approach for indexing groundwater heavy metal pollution. *Ecol Indic* 87:323–331
- Chen L, Liang S, Liu MD, Yi YJ, Mi ZF, Zhang YX, Li YM, Qi JC, Meng J, Tang X, Zhang HR, Tong YD, Zhang W, Wang XJ, Shu J, Yang ZF (2019) Trans-provincial health impacts of atmospheric mercury emissions in China. *Nat Commun* 10:1484
- Dash S, Borah SS, Kalamdhad AS (2020) Application of positive matrix factorization receptor model and elemental analysis for the assessment of sediment contamination and their source apportionment of Deepor Beel, Assam. *Ecol Indic, India*, p 114
- Franco-Uria A, Lopez-Mateo C, Roca E, Fernandez-Marcos ML (2009) Source identification of heavy metals in pastureland by multivariate analysis in NW Spain. *J Hazard Mater* 165:1008–1015
- Guo BX, Liu YQ, Zhang F, Hou JZ, Zhang HB, Li CL (2018) Heavy metals in the surface sediments of lakes on the Tibetan Plateau, China. *Environ Sci Pollut Res* 25:3695–3707



- Hakanson L (1980) An ecological risk index for aquatic pollution control. a sedimentological approach. *Water Res* 14:975–1001
- Hong AH, Hargan KE, Williams B, Nuangsaeng B, Siritwong S, Tasawad P, Chaiarn C, Los Huertos M (2020) Examining molluscs as bioindicators of shrimp aquaculture effluent contamination in a southeast Asian mangrove. *Ecol Indic* 115:106365
- Huang ZF, Liu CY, Zhao XR, Dong J, Zheng BH (2020) Risk assessment of heavy metals in the surface sediment at the drinking water source of the Xiangjiang River in South China. *Environ Sci Eur* 32:1–9
- Islam MS, Proshad R, Ahmed S (2018) Ecological risk of heavy metals in sediment of an urban river in Bangladesh. *Hum Ecol Risk Assess* 24:699–720
- Jiang YF, Guo X (2019) Multivariate and geostatistical analyses of heavy metal pollution from different sources among farmlands in the Poyang Lake region. *China J Soils Sediments* 19:2472–2484
- Jiang YX, Chao SH, Liu JW, Yang Y, Chen YJ, Zhang AC, Cao HB (2017) Source apportionment and health risk assessment of heavy metals in soil for a township in Jiangsu Province, China. *Chemosphere* 168:1658–1668
- Jin YL, O'Connor D, Ok YS, Tsang DCW, Liu A, Hou DY (2019) Assessment of sources of heavy metals in soil and dust at children's playgrounds in Beijing using GIS and multivariate statistical analysis. *Environ Int* 124:320–328
- Karimi-Maleh H, Ayati A, Ghanbari S, Orooji Y, Tanhaei B, Karimi F, Alizadeh M, Rouhi J, Fu L, Sillanpaa M (2021) Recent advances in removal techniques of Cr(VI) toxic ion from aqueous solution: a comprehensive review. *J Mol Liq* 329:115062
- Li HM, Kang XM, Li XM, Li Q, Song JM, Jiao NZ, Zhang YY (2017) Heavy metals in surface sediments along the Weihai coast, China: distribution, sources and contamination assessment. *Mar Pollut Bull* 115:551–558
- Li YY, Gao B, Xu DY, Peng WQ, Liu XB, Qu XD, Zhang M (2020) Hydrodynamic impact on trace metals in sediments in the cascade reservoirs, North China. *Sci Total Environ* 716:136914
- Lin Q, Liu EF, Zhang EL, Li K, Shen J (2016) Spatial distribution, contamination and ecological risk assessment of heavy metals in surface sediments of Erhai Lake, a large eutrophic plateau lake in southwest China. *Catena* 145:193–203
- Liu JL, Li YL, Zhang B, Cao JL, Cao ZG, Domagalski J (2009) Ecological risk of heavy metals in sediments of the Luan River source water. *Ecotoxicology* 18:748–758
- Maanan M, Saddik M, Maanan M, Chaibi M, Assobhei O, Zou-rarah B (2015) Environmental and ecological risk assessment of heavy metals in sediments of Nador lagoon, Morocco. *Ecol Indic* 48:616–626
- Mendiguchía C, Moreno C, Mánuel-Vez MP, García-Vargas M (2006) Preliminary investigation on the enrichment of heavy metals in marine sediments originated from intensive aquaculture effluents. *Aquaculture* 254:317–325
- Mirzaei M, Hatamimanes M, Haghshenas A, Moghaddam SM, Ozunu A, Azadi H (2020) Spatial-seasonal variations and ecological risk of heavy metals in Persian gulf coastal region: case study of Iran. *J Environ Health Sci* 18:91–105
- Rodriguez Martin JA, Arias ML, GrauCorbi JM (2006) Heavy metals contents in agricultural topsoils in the Ebro basin (Spain). Application of the multivariate geostatistical methods to study spatial variations. *Environ Pollut (Barking, Essex: 1987)* 144:1001–12
- Sundaray SK, Nayak BB, Lin S, Bhatta D (2011) Geochemical speciation and risk assessment of heavy metals in the river estuarine sediments-A case study: Mahanadi basin. *India J Hazard Mater* 186:1837–1846
- Tian K, Wu QM, Liu P, Hu WY, Huang B, Shi B, Zhou YQ, Kwon BO, Choi K, Ryu J, Khim JS, Wang TY (2020) Ecological risk assessment of heavy metals in sediments and water from the coastal areas of the Bohai Sea and the Yellow Sea. *Environ Int* 136:105512
- Tunca E, Aydin M, Sahin UA (2018) An ecological risk investigation of marine sediment from the northern Mediterranean coasts (Aegean Sea) using multiple methods of pollution determination. *Environ Sci Pollut Res* 25:7487–7503
- Wang YZ, Duan XJ, Wang L (2020) Spatial distribution and source analysis of heavy metals in soils influenced by industrial enterprise distribution: Case study in Jiangsu Province. *Sci Total Environ* 710:134953
- Xia WT, Wang R, Zhu B, Rudstam LG, Liu YL, Xu YX, Xin W, Chen YS (2020) Heavy metal gradients from rural to urban lakes in central China. *Ecol Process* 9:1
- Xiao R, Bai JH, Huang LB, Zhang HG, Cui BS, Liu XH (2013) Distribution and pollution, toxicity and risk assessment of heavy metals in sediments from urban and rural rivers of the Pearl River delta in southern China. *Ecotoxicology* 22:1564–1575
- Yan CY, Zhuang T, Bai JH, Wen XJ, Lu QQ, Zhang L (2020) Assessment of As, Cd, Zn, Cu and Pb Pollution and Toxicity in River Wetland Sediments and Artificial Wetland Soils Affected by Urbanization in a Chinese Delta. *Wetlands* 40:2799–2809
- Yi YJ, Sun J, Tang CH, Zhang SH (2016) Ecological risk assessment of heavy metals in sediment in the upper reach of the Yangtze River. *Environ Sci Pollut Res* 23:11002–11013
- Zhang ZX, Karimi-Maleh H (2023a) In situ synthesis of label-free electrochemical aptasensor-based sandwich-like AuNPs/PPy/Ti3C2Tx for ultrasensitive detection of lead ions as hazardous pollutants in environmental fluids. *Chemosphere* 324:138302
- Zhang ZX, Karimi-Maleh H (2023b) Label-free electrochemical aptasensor based on gold nanoparticles/titanium carbide MXene for lead detection with its reduction peak as index signal. *Adv Compos Hybrid Mater* 6:68
- Zhang C, Shan BQ, Tang WZ, Dong LX, Zhang WQ, Pei YS (2017) Heavy metal concentrations and speciation in riverine sediments and the risks posed in three urban belts in the Haihe Basin. *Ecotox Environ Safe* 139:263–271

**Publisher's Note** Springer Nature remains neutral with regard to jurisdictional claims in published maps and institutional affiliations.

Springer Nature or its licensor (e.g. a society or other partner) holds exclusive rights to this article under a publishing agreement with the author(s) or other rightsholder(s); author self-archiving of the accepted manuscript version of this article is solely governed by the terms of such publishing agreement and applicable law.